Magnetocrystalline and magnetoelastic constants determined by magnetization dynamics under static strain

J-y Duquesne, P. Rovillain, C. Hepburn, Massimiliano Marangolo

Magnetocrystalline and magnetoelastic constants determined by magnetization dynamics under static strain

J.-Y. Duquesne, C. Hepburn, P. Rovillain, M. Marangolo

Sorbonne Université, CNRS, Institut des Nanosciences de Paris (UMR 7588), 4 place Jussieu, 75252 Paris, France

Abstract. We consider here the magnetization dynamics induced in a ferromagnet by magnetoelastic coupling, after application of a step like strain. We derive the time evolution of the magnetization vector. We show that the material micromagnetic parameters (and specifically magnetic anisotropy and magnetoelastic coupling) can be derived from measurable quantities, i.e. the precession frequency, relaxation time and phase lag between the precession angles. Such measurements can be performed by state of the art time resolved Kerr experiments.

Keywords magnetoelasticity, magnetic anisotropy, time resolved Kerr effect, thin magnetic films, magnetization dynamics

1. Introduction

Recently, much effort has been devoted to control magnetization in nanostructures by external stress and subsequent strain, i.e. the so-called straintronics [1, 2]. Indeed, it is claimed that spintronics devices whose magnetization is switched by strain rather than by inductive means may lead to significant energy dissipation reduction. When a ferromagnetic material is deformed by an external stress it inevitably experiences a change of its magnetic configuration. This is the well-known inverse magnetostriction (or Villari) effect whereby an effective inner magnetic field originating from an external stress modifies the equilibrium direction of the sample's magnetization $\boldsymbol{M}$. The magnetization dynamics is dictated by the torque that makes the magnetization precess around the magnetic field $\boldsymbol{B}$, similarly to a top spinning around the gravitational force. The magnetization moves from the initial equilibrium position to the final one following an oscillating motion whose characteristics are determined by the external applied field, by the intensity of the applied stress and by intrinsic physical properties of the sample such as $|\boldsymbol{M}|$, magnetic anisotropy and magnetoelastic coupling. Due to damping, the final equilibrium position will coincide with the direction of the total field, i.e. the external field plus the stress-induced one. In this sense, we can state that magnetization dynamics is triggered by the sudden application of a constant strain. In straintronics devices, magnetization reversal is required in order to modify significantly the status

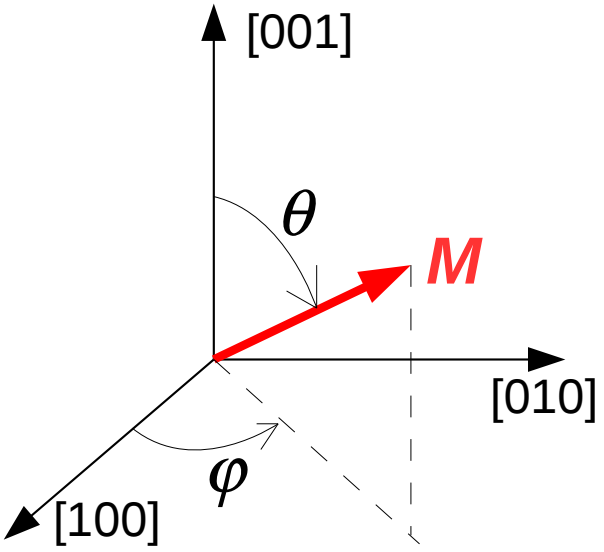

Figure 1. Spherical coordinates φ and θ of the magnetization $\boldsymbol{M}$

of the spintronic device. In this context, the temporal evolution of the magnetization vector of a single-domain nanomagnet is ruled by the non-linear Landau-Lifshitz-Gilbert (LLG) equation.

Here, we study the motion in the case of a weak perturbation of the magnetization due to a sudden deformation of a thin film. We assume that the changes of magnetization direction induced by the applied strain are very small, permitting a linear approximation of the LLG equations. Recently, this approach has been adopted in continuous thin films to describe precession triggering due to an acoustic wave [3, 4]. In this article, we consider a step-like static deformation (ideally, a Heaviside step deformation) and we derive the analytical description of the magnetization motion. Interestingly, we show that by monitoring the magnetization dynamics induced by this deformation it is possible to measure the magnetic anisotropy coefficients and magnetoelastic coupling parameters. Well known methods to extract the magnetocrystalline coefficients are ferromagnetic resonance (FMR) and Brillouin scattering (BLS). Recently, an optical pump-probe method has been described and used [5]. Unfortunately, these methods do not provide information about the magnetoelastic parameters. These terms can be measured by cantilever method [6, 7]. Here, we propose a new method to retrieve both magnetocrystalline and magnetoelastic parameters. It is close to the aforementioned optical pump-probe experiment but here magnetodynamics is triggered by strain and not by an optical laser pulse.

2. Energy terms

In this article, we focus on ferromagnetic thin films on piezoelectric substrates. We consider the thin film as monocrystalline with cubic symmetry. Similar calculations can

be performed in systems exhibiting different crystalline symmetries. The magnetization $\boldsymbol{M}$ and the applied magnetic field $\boldsymbol{H_a}$ are expressed in polar coordinates (with coordinate axes aligned along the $\langle 100 \rangle$ directions) as follows (see figure 1)

$$\boldsymbol{M} = M \begin{pmatrix} \sin\theta \ \cos\varphi \\ \sin\theta \ \sin\varphi \\ \cos\theta \end{pmatrix} \tag{1}$$

$$\boldsymbol{H}_a = H_a \begin{pmatrix} \sin\theta_H \ \cos\varphi_H \\ \sin\theta_H \ \sin\varphi_H \\ \cos\theta_H \end{pmatrix} \tag{2}$$

The free energy density of the system can be written as follows:

$$F = F_z + F_d + F_{mc} + F_{ms} + F_{el} \tag{3}$$

where the first term on the right hand side is the Zeeman energy:

$$\begin{aligned} F_z &= -\mu_0 \boldsymbol{H}_a \boldsymbol{M} \\ &= -\mu_0 H_a M \left[\cos\theta\cos\theta_H \right. \\ &\quad \left. + \sin\theta\sin\theta_H\cos(\varphi - \varphi_H)\right] \end{aligned} \tag{4}$$

The second term expresses the magnetic energy associated with the demagnetizing field in thin films:

$$F_d = \frac{1}{2}\mu_0 M^2 \cos^2\theta \tag{5}$$

The third term is the biaxial cubic magnetocrystalline energy with constant K and direction cosines of the magnetization m_i:

$$F_{mc} = K\left(m_x^2 m_y^2 + m_x^2 m_z^2 + m_y^2 m_z^2\right) \tag{6}$$

The fourth term is the cubic magnetoelastic energy determined by the magnetoelastic constants B_1 and B_2 [8]:

$$\begin{aligned} F_{ms} = \ & B_1\left[\varepsilon_{xx}(m_x^2 - \tfrac{1}{3}) + \varepsilon_{yy}(m_y^2 - \tfrac{1}{3}) + \varepsilon_{zz}(m_z^2 - \tfrac{1}{3})\right] \\ & + B_2\left[\varepsilon_{xy}m_x m_y + \varepsilon_{xz}m_x m_z + \varepsilon_{yz}m_y m_z\right] \end{aligned} \tag{7}$$

The fifth term is the elastic term for a cubic system characterized by the elastic constants C_{ij}:

$$\begin{aligned} F_{el} &= \tfrac{1}{2}C_{11}\left(\varepsilon_{xx}^2 + \varepsilon_{yy}^2 + \varepsilon_{zz}^2\right) \\ &\quad + 2C_{44}\left(\varepsilon_{xy}^2 + \varepsilon_{xz}^2 + \varepsilon_{yz}^2\right) \\ &\quad + C_{12}\left(\varepsilon_{xx}\varepsilon_{yy} + \varepsilon_{xx}\varepsilon_{zz} + \varepsilon_{yy}\varepsilon_{zz}\right) \end{aligned} \tag{8}$$

In (7) and (8), the ε_{ij} are the components of the strain tensor. By minimizing the free energy of the system with respect to θ, φ and ε_{ij}, the equilibrium values of the magnetization angles $\bar{\theta}$ and $\bar{\varphi}$ and of the strain tensor components $\bar{\varepsilon}_{ij}$ are derived (see Appendix A).

In the following, the magnetization and strain subscripts x, y and z will be replaced by 1, 2 and 3, respectively, in order to simplify the mathematical expressions.

3. Dynamical equations for a magnetic system prone to a strain

Let us consider a single domain ferromagnet characterized by its equilibrium magnetization vector $\boldsymbol{M}$ and internal strain. This system is prone to a static or to a dynamical deformation expressed by a strain tensor, $\delta\varepsilon_{ij}(t)$, superimposed on the static equilibrium strain. The response of magnetization to the modified internal field is described by the Landau-Lifschitz-Gilbert (LLG) equations:

$$\frac{d\boldsymbol{m}}{dt} = -\,\gamma\ \boldsymbol{m}\times\boldsymbol{B}_{eff} + \alpha\ \boldsymbol{m}\times\frac{d\boldsymbol{m}}{dt} \tag{9}$$

where

$$\boldsymbol{m} = \frac{\boldsymbol{M}}{M} \tag{10}$$

$$\boldsymbol{B}_{eff} = -\nabla_{\boldsymbol{m}} f \tag{11}$$

$$f = \frac{F}{M} \tag{12}$$

γ is the absolute value of the gyromagnetic factor and α is the Gilbert damping coefficient. M is the saturation value of the magnetization ($M = |\boldsymbol{M}|$). In the polar coordinate system, the LLG equations read (taking into account that $\boldsymbol{m}$ does not depend on the radial coordinate):

$$\begin{cases} \dfrac{d\varphi}{dt} &= +\dfrac{\gamma}{\sin\theta}\dfrac{\partial f}{\partial\theta} + \dfrac{\alpha}{\sin\theta}\dfrac{d\theta}{dt} \\ \dfrac{d\theta}{dt} &= -\dfrac{\gamma}{\sin\theta}\dfrac{\partial f}{\partial\varphi} - \alpha\sin\theta\dfrac{d\varphi}{dt} \end{cases} \tag{13}$$

leading to:

$$\begin{cases} \dfrac{d\varphi}{dt} &= \dfrac{\gamma}{1+\alpha^2}\dfrac{1}{\sin\theta}\dfrac{\partial f}{\partial\theta} - \dfrac{\alpha\gamma}{1+\alpha^2}\dfrac{1}{\sin^2\theta}\dfrac{\partial f}{\partial\varphi} \\ \dfrac{d\theta}{dt} &= -\dfrac{\alpha\gamma}{1+\alpha^2}\dfrac{\partial f}{\partial\theta} - \dfrac{\gamma}{1+\alpha^2}\dfrac{1}{\sin\theta}\dfrac{\partial f}{\partial\varphi} \end{cases} \tag{14}$$

We consider that the magnetization vector $\boldsymbol{M}$ is only slightly modified by the external strain perturbation, so that we can linearize the LLG equation (14) about equilibrium [3, 4]. It can be show that this condition is fullfilled when $|B\varepsilon| << |K|$ where B is B_1 or B_2 and ε the sample strain. The $\frac{\partial f}{\partial\theta}$, $\frac{1}{\sin\theta}\frac{\partial f}{\partial\theta}$, $\frac{1}{\sin\theta}\frac{\partial f}{\partial\varphi}$ and $\frac{1}{\sin^2\theta}\frac{\partial f}{\partial\varphi}$ functions (which depend on θ, φ, ε_{11}, ε_{12}, ε_{13}, ε_{22}, ε_{23} and ε_{33}) are then expressed as Taylor series about equilibrium ($\bar{\theta}$, $\bar{\varphi}$, $\bar{\varepsilon}_{ij}$). Since the first order derivatives of f are zero at equilibrium, the

expansion yields:

$$\begin{cases} \dfrac{\partial f}{\partial \theta} & \simeq & f_{\theta,\theta}\ \delta\theta + \ f_{\theta,\varphi}\ \delta\varphi + \displaystyle\sum_{i\leq j}\ f_{\theta,\varepsilon_{ij}}\delta\varepsilon_{ij} \\ \dfrac{1}{\sin\theta}\dfrac{\partial f}{\partial \theta} & \simeq & \dfrac{1}{\sin\bar{\theta}}\ f_{\theta,\theta}\ \delta\theta + \dfrac{1}{\sin\bar{\theta}}\ f_{\theta,\varphi}\ \delta\varphi \\ & & + \dfrac{1}{\sin\bar{\theta}}\displaystyle\sum_{i\leq j}\ f_{\theta,\varepsilon_{ij}}\delta\varepsilon_{ij} \\ \dfrac{1}{\sin\theta}\dfrac{\partial f}{\partial \varphi} & \simeq & \dfrac{1}{\sin\bar{\theta}}\ f_{\theta,\varphi}\ \delta\theta + \dfrac{1}{\sin\bar{\theta}}\ f_{\varphi,\varphi}\ \delta\varphi \\ & & + \dfrac{1}{\sin\bar{\theta}}\displaystyle\sum_{i\leq j}\ f_{\varphi,\varepsilon_{ij}}\delta\varepsilon_{ij} \\ \dfrac{1}{\sin^2\theta}\dfrac{\partial f}{\partial \varphi} & \simeq & \dfrac{1}{\sin^2\bar{\theta}}\ f_{\theta,\varphi}\ \delta\theta + \dfrac{1}{\sin^2\bar{\theta}}\ f_{\varphi,\varphi}\ \delta\varphi \\ & & + \dfrac{1}{\sin^2\bar{\theta}}\displaystyle\sum_{i\leq j}\ f_{\varphi,\varepsilon_{ij}}\delta\varepsilon_{ij} \end{cases} \tag{15}$$

where $f_{a,b}$ is a short hand notation for $\frac{\partial^2 f}{\partial a \partial b}$. The second order derivatives $f_{a,b}$ are to be evaluated at the equilibrium point ($\bar{\theta}$, $\bar{\varphi}$, $\bar{\varepsilon}_{11}$, $\bar{\varepsilon}_{12}$, $\bar{\varepsilon}_{13}$, $\bar{\varepsilon}_{22}$, $\bar{\varepsilon}_{23}$ and $\bar{\varepsilon}_{33}$). $\delta\theta$ and $\delta\varphi$ are the deviations from the equilibrium angles $\bar{\theta}$ and $\bar{\varphi}$. $\delta\varepsilon_{ij}$ are the deviations from equilibrium values $\bar{\varepsilon}_{ij}$:

$$\delta\theta = \theta - \bar{\theta} \tag{16}$$

$$\delta\varphi = \varphi - \bar{\varphi} \tag{17}$$

$$\delta\varepsilon_{ij} = \varepsilon_{ij} - \bar{\varepsilon}_{ij} \tag{18}$$

Plugging these expansions in (14) gives:

$$\begin{cases} \dfrac{d\delta\varphi}{dt} & = & \kappa_1\ \delta\theta + \kappa_2\ \delta\varphi + \displaystyle\sum_{i\leq j}\kappa_{ij}\ \delta\varepsilon_{ij} \\ \dfrac{d\delta\theta}{dt} & = & \zeta_1\ \delta\theta + \zeta_2\ \delta\varphi + \displaystyle\sum_{i\leq j}\zeta_{ij}\ \delta\varepsilon_{ij} \end{cases} \tag{19}$$

The energy second derivatives, the κ and ζ terms are given in Appendix B, in the case of a thin film, with in-plane magnetization, and in-plane applied field.

4. Analytical solutions for the magnetization motion. Case of a step-like static strain

Now, we consider a step-like deformation. At $t = 0$, a strain is suddenly applied: $\delta\varepsilon_{ij}(t) = \delta\varepsilon_{ij}\Theta(t)$ where Θ is the Heaviside step function. Because of the internal

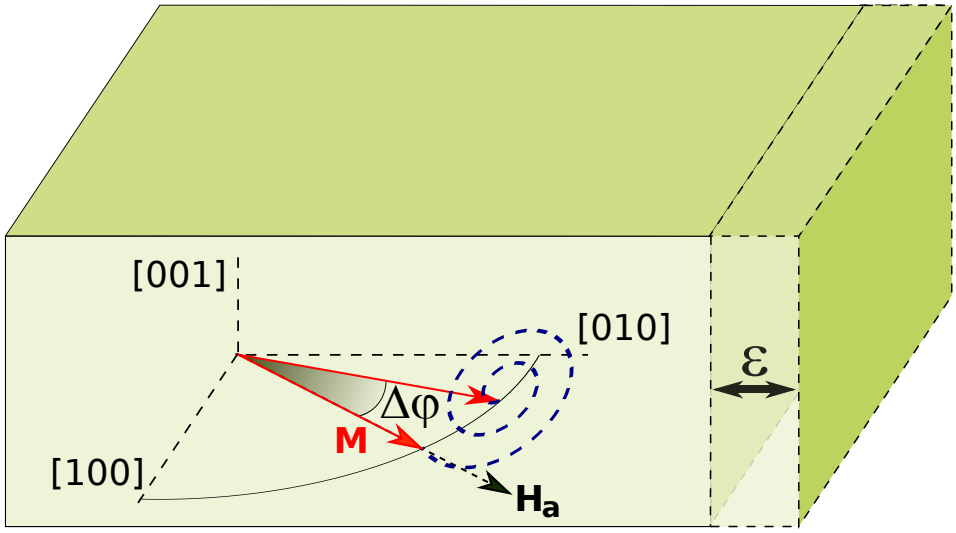

Figure 2. Sketch of the damped precessional motion of the magnetization $\boldsymbol{M}$, in response to a sudden static strain ε. Initial and final magnetization in plane (001). Tensile/compressive strain ε along [010].

effective field $\boldsymbol{B}_{eff}$ applied to the single domain, the direction of the magnetization vector $\boldsymbol{M}$ will be modified. Following a damped oscillatory motion, the magnetization angles θ and φ will converge towards the new equilibrium values $\bar{\bar{\theta}}$ and $\bar{\bar{\varphi}}$. Figure 2 shows a sketch of the precessional motion of the magnetization. The movement will finally stop and, according to (19), the new equilibrium will satisfy:

$$\left\{\begin{array}{rcl} 0 & = & \kappa_1\ (\bar{\bar{\theta}}-\bar{\theta}) + \kappa_2\ (\bar{\bar{\varphi}}-\bar{\varphi}) + \sum\limits_{i\leq j} \kappa_{ij}\ \delta\varepsilon_{ij} \\ 0 & = & \zeta_1\ (\bar{\bar{\theta}}-\bar{\theta}) + \zeta_2\ (\bar{\bar{\varphi}}-\bar{\varphi}) + \sum\limits_{i\leq j} \zeta_{ij}\ \delta\varepsilon_{ij} \end{array}\right. \tag{20}$$

Substracting (19) and (20), we obtain:

$$\frac{d}{dt}\begin{pmatrix} \varphi-\bar{\bar{\varphi}} \\ \theta-\bar{\bar{\theta}} \end{pmatrix} = P \begin{pmatrix} \varphi-\bar{\bar{\varphi}} \\ \theta-\bar{\bar{\theta}} \end{pmatrix} \tag{21}$$

where

$$P = \begin{pmatrix} \kappa_2 & \kappa_1 \\ \zeta_2 & \zeta_1 \end{pmatrix} \tag{22}$$

The time dependent solutions for φ and θ are:

$$\begin{pmatrix} \varphi-\bar{\bar{\varphi}} \\ \theta-\bar{\bar{\theta}} \end{pmatrix} = \beta_1 e^{\lambda_1 t}\boldsymbol{U_1} + \beta_2 e^{\lambda_2 t}\boldsymbol{U_2} \tag{23}$$

where λ_1 et λ_2 are the eigenvalues of the P matrix and $\boldsymbol{U_1}$ et $\boldsymbol{U_2}$ the corresponding eigenvectors. By an elementary calculation we obtain:

$$\begin{array}{rcl} \lambda_1 & = & -\tau^{-1} - i\ \Omega_0 \\ \lambda_2 & = & -\tau^{-1} + i\ \Omega_0 \end{array} \tag{24}$$

Table 1. Characteristics of YIG and $Fe_{80}Ga_{20}$ thin films, with in-plane equilibrium magnetization: threshold field $\mu_0 H_{th}$, precession angular frequency Ω_0 and damping time τ. Ω_0 and τ are computed using $\mu_0 H_a = 38$ mT (in-plane applied field). τ is nearly independent of H_a. Material parameters: see Appendix D.

		YIG			$Fe_{80}Ga_{20}$		
φ_H (rd)	$\bar{\varphi}$ (rd)	$\mu_0 H_{th}$ (mT)	Ω_0 (rd.s^{-1})	τ (ns)	$\mu_0 H_{th}$ (mT)	Ω_0 (rd.s^{-1})	τ (ns)
$\pi/4$	$\pi/4$	0	17×10^9	193	35	14×10^9	1.25
0	0	9	2.2×10^9	211	0	68×10^9	1.18

$$\boldsymbol{U}_1 = \begin{pmatrix} 1 \\ -\frac{1}{2}\alpha\left(1 - \frac{f_{\varphi,\varphi}}{f_{\theta,\theta}}\right) - i\ \frac{1+\alpha^2}{\gamma f_{\theta,\theta}}\ \Omega_0 \end{pmatrix} \tag{25}$$

$$\boldsymbol{U}_2 = \begin{pmatrix} 1 \\ -\frac{1}{2}\alpha\left(1 - \frac{f_{\varphi,\varphi}}{f_{\theta,\theta}}\right) + i\ \frac{1+\alpha^2}{\gamma f_{\theta,\theta}}\ \Omega_0 \end{pmatrix} \tag{26}$$

with:

$$\Omega_0 = \sqrt{\left(\frac{1}{1+\alpha^2}\right)\omega_0^2 - \tau^{-2}} \tag{27}$$

$$\omega_0 = \gamma\sqrt{f_{\theta,\theta} f_{\varphi,\varphi}} \tag{28}$$

$$\tau^{-1} = \frac{1}{2}\frac{\alpha\gamma}{1+\alpha^2}(f_{\theta,\theta} + f_{\varphi,\varphi}) \tag{29}$$

Ω_0, ω_0 and τ are characteristics of the eigen mode [4]: damped and undamped radial frequencies and relaxation time, respectively. The reader has to notice that in a ferromagnetic material, Ω_0 is found to be real for external fields larger than a threshold values H_{th}, leading to complex eigenvalues and a damped oscillatory motion starting from $(\bar{\varphi},\ \bar{\theta})$ and ending to $(\bar{\bar{\varphi}},\ \bar{\bar{\theta}})$. Let us consider two paradigmatic materials: YIG, on one hand, with small anisotropy and small magneto-elastic constants and $Fe_{80}Ga_{20}$, on the other hand, with larger anisotropy and larger magneto-elastic constants. It is worthwhile to notice that similar measurements performed on materials with very high magnetic anisotropy demand strong magnetic fields. Let us consider $DyFe_2$ (which is both a highly anisotropic and magnetostrictive material) where $K = 4.2 \times 10^6$ J.m^{-3} [9] and the consequent threshold value is $H_{th} = 11$ T. Even for very low damping ($\alpha \simeq 0.005$), the relaxation time τ will be very short, of the order of 0.1 ns. We will see later that this is a severe constraint for actual measurements.

Table 1 displays characteristics values, for thin films with in plane magnetization. Of course, the more intense the field the larger Ω_0.

The β_1 and β_2 constants are given by the initial conditions. At $t = 0$, we have $\varphi = \bar{\varphi}$

and $\theta = \bar{\theta}$ since the system has not yet evolved. According to (23):

$$\begin{pmatrix} \bar{\varphi} - \bar{\bar{\varphi}} \\ \bar{\theta} - \bar{\bar{\theta}} \end{pmatrix} = \beta_1 \boldsymbol{U_1} + \beta_2 \boldsymbol{U_2} \tag{30}$$

This gives:

$$\begin{aligned} \beta_1 &= \left[-\frac{1}{2} - \frac{1}{4} \frac{\alpha\gamma}{1+\alpha^2} \frac{f_{\theta,\theta} - f_{\varphi,\varphi}}{\Omega_0}\, i \right] \Delta\varphi \\ &\quad -\frac{1}{2} \frac{\gamma}{1+\alpha^2} \frac{f_{\theta,\theta}}{\Omega_0}\, i\, \Delta\theta \end{aligned} \tag{31}$$

$$\begin{aligned} \beta_2 &= \left[-\frac{1}{2} + \frac{1}{4} \frac{\alpha\gamma}{1+\alpha^2} \frac{f_{\theta,\theta} - f_{\varphi,\varphi}}{\Omega_0}\, i \right] \Delta\varphi \\ &+ \frac{1}{2} \frac{\gamma}{1+\alpha^2} \frac{f_{\theta,\theta}}{\Omega_0}\, i\, \Delta\theta \end{aligned} \tag{32}$$

$$\Delta\varphi = \bar{\bar{\varphi}} - \bar{\varphi} \tag{33}$$

$$\Delta\theta = \bar{\bar{\theta}} - \bar{\theta} \tag{34}$$

$\Delta\varphi$ and $\Delta\theta$ are the variation of the equilibrium angles. They can be computed from (20), given the applied strain components $\delta\varepsilon_{ij}$. We now considerer thin magnetic films where the demagnetizing field stabilizes in-plane equilibrium magnetic configurations. Appendix C gives $\Delta\varphi$ and $\Delta\theta$ in three relevant strain cases. Let us assume first that $\Delta\theta = 0$. Using (23), the time dependence of the magnetization angles can be derived straightforwardly. This permits to recover the expected solutions of a simple damped oscillator movement:

$$\varphi - \bar{\bar{\varphi}} = \frac{\omega_0\ \Delta\varphi}{(1+\alpha^2)\Omega_0}\ e^{-t/\tau} \cos(\Omega_0 t - \delta) \tag{35}$$

$$\theta - \bar{\bar{\theta}} = \frac{\gamma f_{\varphi,\varphi}\ \Delta\varphi}{(1+\alpha^2)\Omega_0}\ e^{-t/\tau} \sin(\Omega_0 t) \tag{36}$$

where

$$\tan\delta = \frac{\alpha\gamma\,(f_{\theta,\theta} - f_{\varphi,\varphi})}{2\ (1+\alpha^2)\ \Omega_0} \tag{37}$$

$$\cos\delta < 0 \tag{38}$$

Figure 3 displays the theoretical behavior of φ and θ, computed for thin YIG and $Fe_{80}Ga_{20}$ layers with $\delta\varepsilon_{11} = \varepsilon = 1 \times 10^{-4}$. We stress that such a deformation can not modify significantly the magnetic anisotropy and is consistent with our LLG linearization procedure. These two materials are quite paradigmatic since YIG is a low damping material (long time scale in figure 3-a) and FeGa is a strong magnetoelastic alloy. In $Fe_{80}Ga_{20}$, we assumed a small, iron like, damping term α. Similar expressions can be derived in cases where $\Delta\varphi = 0$. As expected, the movement of magnetization from the initial equilibrium position towards the final external strain-dependent position will follow a damped oscillatory motion characterized by a fast oscillation Ω_0 (the

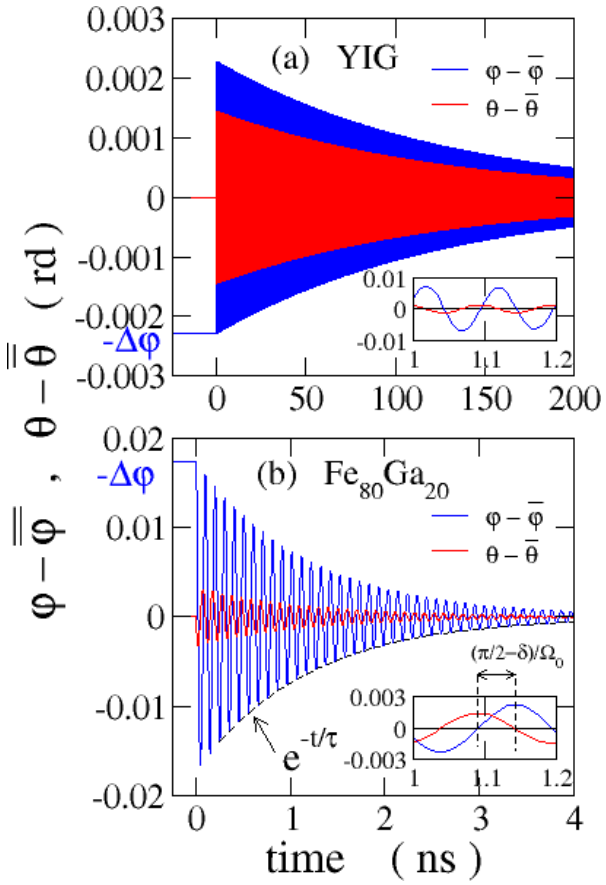

Figure 3. Calculation of the precession angles φ and θ, in response to a tensile strain Heaviside step along [100]. Thin films, normal to [001]. Applied field: 0.1 T along [110] ($\varphi_H = \pi/4$, $\theta_H = \pi/2$). Equilibrium angles: $\bar{\varphi} = \pi/4$, $\bar{\theta} = \pi/2$. Applied strain $\varepsilon = 1 \times 10^{-4}$. Material parameters: see appendix Appendix D. Left panel (a): YIG. $\Omega_0/2\pi = 4.8$ GHz, $\tau = 130$ ns, $\delta = 3.1417$ rd. Right panel (b): $Fe_{80}Ga_{20}$. $\Omega_0/2\pi = 9.8$ GHz, $\tau = 1.2$ ns. $\delta = 3.1545$ rd

ferromagnetic resonance frequency of the magnetic system) modulated by an exponential decay characterized by the relaxation time τ. Moreover, the φ and θ oscillations will be out-of-phase by $(\pi/2 - \delta)$. Interestingly, all these measurable parameters depend on the applied external field and on intrinsic quantities of the ferromagnetic thin films, i.e. the second derivatives $f_{\varphi,\varphi}$ and $f_{\theta,\theta}$ of the free energy evaluated at the initial equilibrium positions of the magnetization.

5. Micromagnetic parameters measurements

In the following we will discuss how magnetic anisotropy parameters K and magnetoelastic coefficients B_1 and B_2 of a thin film can be extracted by monitoring the time dependence of the relaxation process of the magnetization vector prone to a

sudden static strain. From (27, 28, 29, 37), we obtain:

$$\alpha^2 = \frac{(\Omega_0\tau)^{-2} - \tan^2\delta}{1+\tan^2\delta} \tag{39}$$

$$f_{\theta,\theta} = \frac{1+\alpha^2}{\alpha\gamma}\left(\tau^{-1} + \Omega_0\tan\delta\right) \tag{40}$$

$$f_{\varphi,\varphi} = \frac{1+\alpha^2}{\alpha\gamma}\left(\tau^{-1} - \Omega_0\tan\delta\right) \tag{41}$$

According to these equations, the intrinsic characteristics of the sample α, $f_{\theta,\theta}$ and $f_{\varphi,\varphi}$ can be derived from the measurable quantities Ω_0, τ and δ. Hence, $f_{\theta,\theta}$ and $f_{\varphi,\varphi}$ can then be extracted as a function of the in-plane angles $\bar{\varphi}$ and φ_H and compared to their theoretical expressions (see Appendix B):

$$\begin{aligned} f_{\theta,\theta} &= \mu_0 H_a\cos(\bar{\varphi}-\varphi_H) + \mu_0 M \\ &\quad + \tfrac{K}{M}\left(2-\sin^2 2\bar{\varphi}\right) \\ &\quad + 2\tfrac{B_1^2}{M(C_{11}-C_{12})}(\cos^4\bar{\varphi}+\sin^4\bar{\varphi}) \\ &\quad + \tfrac{B_2^2}{8MC_{44}}\sin^2 2\bar{\varphi} \end{aligned} \tag{42}$$

$$\begin{aligned} f_{\varphi,\varphi} &= \mu_0 H_a\cos(\bar{\varphi}-\varphi_H) \\ &\quad + 2\tfrac{K}{M}\cos 4\bar{\varphi} \\ &\quad + 2\tfrac{B_1^2}{M(C_{11}-C_{12})}\cos^2 2\bar{\varphi} \\ &\quad + \tfrac{B_2^2}{4MC_{44}}\sin^2 2\bar{\varphi} \end{aligned} \tag{43}$$

It is cumbersome to determine the equilibrium angle $\bar{\varphi}$, for an arbitrary field. Hence, we assume that we apply an in-plane external field $\boldsymbol{H}$ strong enough to saturate the sample along the field, i.e. $\bar{\varphi} = \varphi_H$ (φ_H is the angle between $\boldsymbol{H}$ and the crystal axis [100]). From an experimental point of view, Ω_0, τ and δ are recorded as a function of φ_H. In order to retrieve K, $|B_1|$ and $|B_2|$ with good accuracy, many measurements angles are considered and a regression analysis of $f_{\theta,\theta}$ and $f_{\varphi,\varphi}$ can be performed by fitting the experimental records to their theoretical expressions. We notice that the signs of B_1 and B_2 can be inferred from the signs of $\Delta\theta = \bar{\bar{\theta}} - \bar{\theta}$ and $\Delta\varphi = \bar{\bar{\varphi}} - \bar{\varphi}$, provided the sign of ε is known (see table C1 in Appendix C). Figure 4 displays $f_{\varphi,\varphi}$ and $f_{\theta,\theta}$ versus φ_H, computed using YIG and $Fe_{80}Ga_{20}$ parameters (black circles). It also displays the modifications induced by parameters changes. These simulations permit to enlighten the contributions of K, B_1 and B_2 to $f_{\varphi,\varphi}$ and $f_{\theta,\theta}$. In particular, K plays an important role for both materials ; B_1 gives an important contribution in magnetoelastic FeGa. It appears that B_2 cannot be retrieved by fitting $f_{\varphi,\varphi}$ and $f_{\theta,\theta}$, because its contribution to those terms is negligeable with respect to the B_1 term contribution. Indeed, direct measurements of B_1 and B_2 could be performed by measuring the absolute magnitude of the φ and θ oscillations. According to Appendix C, tensile or compressive strain along [100] and along [110] will induce amplitudes quasi-proportional to B_1 and B_2,

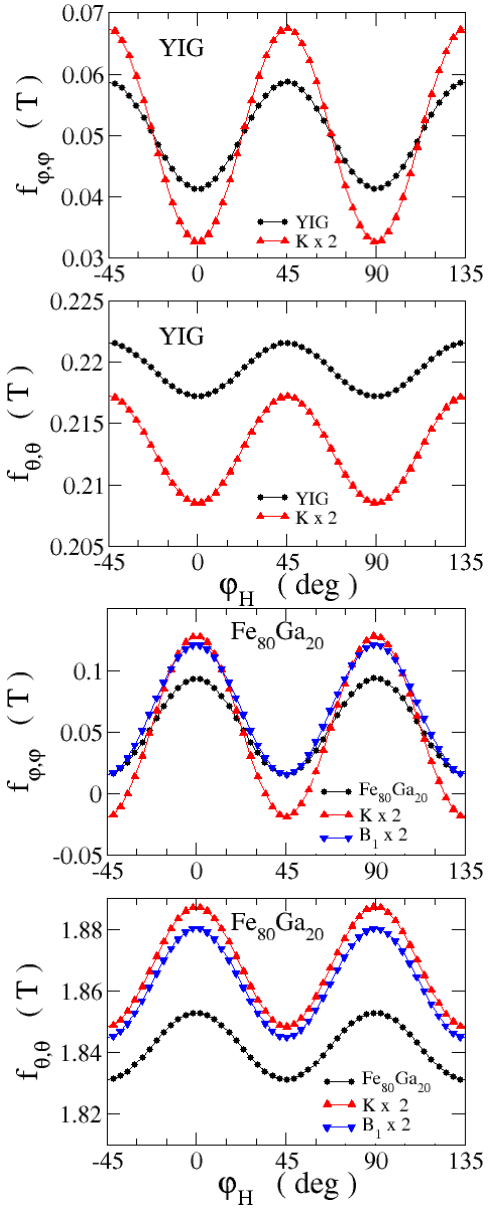

Figure 4. $f_{\varphi,\varphi}$ and $f_{\theta,\theta}$ versus the in-plane applied field angle φ_H for YIG and $Fe_{80}Ga_{20}$ thin films. The applied field (50 mT) is large enough to align the magnetization along the field ($\bar{\varphi} = \varphi_H$). Black circles : YIG and $Fe_{80}Ga_{20}$ parameters (see Appendix D). Red up triangles and blue down triangles curves are computed for modified K or B_1 values, as indicated in the panels. Materials parameters: see Appendix D.

respectively.

From an experimental point of view, the strain is to be applied by means of the piezoelectric substrate on which the thin ferromagnetic layer is attached. When submitted to a voltage, the substrate will strain the film. Indeed, the experiment demands a sudden strain modification, ideally the Heaviside strain step. In actual experiments, it can be replaced by a rapid strain modification, on a time scale shorter than the relaxation time τ. It can be shown that, after a transient regime, (35) and (36) are recovered. The time dependence of the φ and θ angles can be recorded by time-resolved magneto-optical polar Kerr effect (TR-MOKE) experiments, synchronized to the applied strain, in the longitudinal and polar configurations, respectively (see for example [10] or [11]). This experiment opens a new way to characterize magnetic anisotropies and magnetoelastic properties of ferromagnetic materials.

6. Conclusion

We have studied the magnetization dynamical response of a thin film when suddenly strained. The dynamics is characterized by damped oscillations and phase lag of the polar and azimuthal angles. Measuring Ω_0, τ and δ by time-resolved magneto-optical experiments, as a function of the angle of the external saturating field (applied in the film plane) provides a new way to measure the micromagnetic parameters K, B_1 and B_2. The method presented in this article could be an alternative way to measure the magnetoelastic parameters. If compared with the cantilever method [6, 7], we notice that both magneto-crystalline and magneto-elastic constants can be retrieved. If compared with the optical pump-probe set-up [5], our method avoids the difficulties of handling two laser beams and avoids heating of the sample.

Acknowledgments

The authors wish to thank L.Thevenard and C.Gourdon for the careful reading of the article and J.Milano for the FMR measurement of FeGa thin films.

Appendix A. Equilibrium strains $\bar{\varepsilon}_{ij}$

At equilibrium, the strain derivatives of the free energy are zero. Then, we obtain a set of 6 equations:

$$\frac{\partial F}{\partial \varepsilon_{ij}} = 0 \tag{A.1}$$

where i and j are in (1,2,3) (and $i \leq j$), leading to (bars denotes the equilibrium values) :

$$\begin{cases} C_{11}\bar{\varepsilon}_{11} + C_{12}\bar{\varepsilon}_{22} + C_{12}\bar{\varepsilon}_{33} &= -B_1(\bar{m}_1^2 - \frac{1}{3}) \\ C_{12}\bar{\varepsilon}_{11} + C_{11}\bar{\varepsilon}_{22} + C_{12}\bar{\varepsilon}_{33} &= -B_1(\bar{m}_2^2 - \frac{1}{3}) \\ C_{12}\bar{\varepsilon}_{11} + C_{12}\bar{\varepsilon}_{22} + C_{11}\bar{\varepsilon}_{33} &= -B_1(\bar{m}_3^2 - \frac{1}{3}) \\ 4\ C_{44}\bar{\varepsilon}_{12} &= -B_2\bar{m}_1\bar{m}_2 \\ 4\ C_{44}\bar{\varepsilon}_{13} &= -B_2\bar{m}_1\bar{m}_3 \\ 4\ C_{44}\bar{\varepsilon}_{23} &= -B_2\bar{m}_2\bar{m}_3 \end{cases} \tag{A.2}$$

Hence:

$$\begin{cases} \bar{\varepsilon}_{ii} &= -\dfrac{B_1}{C_{11} - C_{12}}\left(\bar{m}_i^2 - \dfrac{1}{3}\right) \\ \\ \bar{\varepsilon}_{ij} &= -\dfrac{B_2}{4C_{44}}\bar{m}_i\bar{m}_j \qquad \text{if} \quad i \neq j \end{cases} \tag{A.3}$$

Notice these equilibrium strain values are written in the standard frame ([100], [010], [001]).

Appendix B. Energy second derivatives, κ and ζ terms

Let us assume the sample is a thin film parallel to the (x,y) plane (with [100], [010], [001] parallel to x, y and z, respectively). We consider in-plane magnetization (i.e. $\bar{m}_3 = 0$ or $\bar{\theta} = \pi/2$) and in-plane applied magnetic field (i.e. $\bar{\theta}_H = \pi/2$). Then, the second order derivatives read:

$$
\begin{cases}
f_{\theta,\theta} &= \mu_0 H_a \cos(\bar{\varphi} - \varphi_H) + \mu_0 M \\
&\quad + \frac{K}{M}\left(2 - \sin^2 2\bar{\varphi}\right) \\
&\quad - 2\frac{B_1}{M}\left(\bar{\varepsilon}_{11}\cos^2\bar{\varphi} + \bar{\varepsilon}_{22}\sin^2\bar{\varphi} - \bar{\varepsilon}_{33}\right) \\
&\quad - \frac{B_2}{M}\bar{\varepsilon}_{12}\sin 2\bar{\varphi} \\
f_{\varphi,\varphi} &= \mu_0 H_a \cos(\bar{\varphi} - \varphi_H) \\
&\quad + 2\frac{K}{M}\cos 4\bar{\varphi} \\
&\quad + 2\frac{B_1}{M}(-\bar{\varepsilon}_{11} + \bar{\varepsilon}_{22})\cos 2\bar{\varphi} \\
&\quad - 2\frac{B_2}{M}\bar{\varepsilon}_{12}\sin 2\bar{\varphi} \\
f_{\theta,\varphi} &= \frac{B_2}{M}\left(\bar{\varepsilon}_{13}\cos\bar{\varphi} - \bar{\varepsilon}_{23}\sin\bar{\varphi}\right) \\
f_{\theta,\varepsilon_{11}} &= 0 \\
f_{\theta,\varepsilon_{22}} &= 0 \\
f_{\theta,\varepsilon_{33}} &= 0 \\
f_{\theta,\varepsilon_{12}} &= 0 \\
f_{\theta,\varepsilon_{13}} &= -\frac{B_2}{M}\cos\bar{\varphi} \\
f_{\theta,\varepsilon_{23}} &= -\frac{B_2}{M}\sin\bar{\varphi} \\
f_{\varphi,\varepsilon_{11}} &= -\frac{B_1}{M}\sin 2\bar{\varphi} \\
f_{\varphi,\varepsilon_{22}} &= \frac{B_1}{M}\sin 2\bar{\varphi} \\
f_{\varphi,\varepsilon_{33}} &= 0 \\
f_{\varphi,\varepsilon_{12}} &= \frac{B_2}{M}\cos 2\varphi \\
f_{\varphi,\varepsilon_{13}} &= 0 \\
f_{\varphi,\varepsilon_{23}} &= 0
\end{cases}
\tag{B.1}
$$

Using the static strain (A.3), $f_{\theta,\theta}$, $f_{\varphi,\varphi}$ and $f_{\theta,\varphi}$ read:

$$\begin{cases} f_{\theta,\theta} &= \mu_0 H_a \cos(\bar{\varphi} - \varphi_H) + \mu_0 M \\ &\quad + \frac{K}{M}\left(2 - \sin^2 2\bar{\varphi}\right) \\ &\quad + 2\frac{B_1^2}{M(C_{11}-C_{12})}(\cos^4\bar{\varphi} + \sin^4\bar{\varphi}) \\ &\quad + \frac{B_2^2}{8MC_{44}}\sin^2 2\bar{\varphi} \\ f_{\varphi,\varphi} &= \mu_0 H_a \cos(\bar{\varphi} - \varphi_H) \\ &\quad + 2\frac{K}{M}\cos 4\bar{\varphi} \\ &\quad + 2\frac{B_1^2}{M(C_{11}-C_{12})}\cos^2 2\bar{\varphi} \\ &\quad + \frac{B_2^2}{4MC_{44}}\sin^2 2\bar{\varphi} \\ f_{\theta,\varphi} &= 0 \end{cases} \tag{B.2}$$

The κ and ζ terms are given by:

$$\begin{cases} \kappa_1 &= \frac{\gamma}{1+\alpha^2} f_{\theta,\theta} \\ \kappa_2 &= -\frac{\alpha\gamma}{1+\alpha^2} f_{\varphi,\varphi} \\ \kappa_{11} &= +\frac{\alpha\gamma}{1+\alpha^2}\frac{B_1}{M}\sin 2\bar{\varphi} \\ \kappa_{12} &= -\frac{\alpha\gamma}{1+\alpha^2}\frac{B_2}{M}\cos 2\bar{\varphi} \\ \kappa_{13} &= -\frac{\gamma}{1+\alpha^2}\frac{B_2}{M}\cos\bar{\varphi} \\ \kappa_{22} &= -\frac{\alpha\gamma}{1+\alpha^2}\frac{B_1}{M}\sin 2\bar{\varphi} \\ \kappa_{23} &= -\frac{\gamma}{1+\alpha^2}\frac{B_2}{M}\sin\bar{\varphi} \\ \kappa_{33} &= 0 \end{cases} \tag{B.3}$$

$$\begin{cases} \zeta_1 &= -\frac{\alpha\gamma}{1+\alpha^2} f_{\theta,\theta} \\ \zeta_2 &= -\frac{\gamma}{1+\alpha^2} f_{\varphi,\varphi} \\ \zeta_{11} &= +\frac{\gamma}{1+\alpha^2}\frac{B_1}{M}\sin 2\bar{\varphi} \\ \zeta_{12} &= -\frac{\gamma}{1+\alpha^2}\frac{B_2}{M}\cos 2\bar{\varphi} \\ \zeta_{13} &= +\frac{\alpha\gamma}{1+\alpha^2}\frac{B_2}{M}\cos\bar{\varphi} \\ \zeta_{22} &= -\frac{\gamma}{1+\alpha^2}\frac{B_1}{M}\sin 2\bar{\varphi} \\ \zeta_{23} &= +\frac{\alpha\gamma}{1+\alpha^2}\frac{B_2}{M}\sin\bar{\varphi} \\ \zeta_{33} &= 0 \end{cases} \tag{B.4}$$

Appendix C. Equilibrium angles $\bar{\bar{\varphi}}$ and $\bar{\bar{\theta}}$

We assume here that the sample is a thin film with in-plane magnetization (same assumptions as in Appendix B). (20) can be easily solved for specific applied strains

$\delta\varepsilon_{ij}$. We consider here three relevant cases, displayed in table C1.

Table C1. Equilibrium angles

	applied strain	$\Delta\theta = \bar{\bar{\theta}} - \bar{\theta}$	$\Delta\varphi = \bar{\bar{\varphi}} - \bar{\varphi}$
uniaxial tensile/compressive strain along [100]	$\begin{pmatrix} \varepsilon & 0 & 0 \\ 0 & 0 & 0 \\ 0 & 0 & 0 \end{pmatrix}$	0	$+\varepsilon \frac{B_1}{M} \frac{\sin 2\bar{\varphi}}{f_{\varphi,\varphi}}$
uniaxial tensile/compressive strain along [110]	$\begin{pmatrix} \varepsilon/2 & \varepsilon/2 & 0 \\ \varepsilon/2 & \varepsilon/2 & 0 \\ 0 & 0 & 0 \end{pmatrix}$	0	$-\frac{\varepsilon}{2} \frac{B_2}{M} \frac{\cos 2\bar{\varphi}}{f_{\varphi,\varphi}}$
x-z shear	$\begin{pmatrix} 0 & 0 & \varepsilon \\ 0 & 0 & 0 \\ \varepsilon & 0 & 0 \end{pmatrix}$	$+\varepsilon \frac{B_2}{M} \frac{\cos \bar{\varphi}}{f_{\theta,\theta}}$	0

Appendix D. Material constants

Table D1 displays the elastic and micromagnetic parameters used for computation.

Table D1. Material constants

	C_{11} (GPa)	C_{12} (GPa)	C_{44} (GPa)	M (A.m^{-1})	α	K (J.m^{-3})	B_1 (J.m^{-3})	B_2 (J.m^{-3})
YIG	269 [12]	76.4 [12]	107.7 [12]	1.4×10^5 [13]	2.3×10^{-4} [14]	-6.10×10^2 [15]	3.48×10^5 [16]	6.96×10^5 [16]
$Fe_{80}Ga_{20}$	196 [17]	156 [17]	123 [17]	14×10^5 [18]	50×10^{-4} [19]	241×10^2 [20]	-160×10^5 [21]	-60×10^5 [21]

References

[1] K. Roy, S. Bandyopadhyay, and J. Atulasimha. Hybrid spintronics and straintronics: A magnetic technology for ultra low energy computing and signal processing. *Appl. Phys. Lett.*, 99:063108, 2011.

[2] H. Ahmad, J. Atulasimha, and S. Bandyopadhyay. Reversible strain-induced magnetization switching in FeGa nanomagnets: pathway to a rewritable, non-volatile, non-toggle, extremely low energy straintronic memory. *Scientific Reports*, 5:18264, 2015.

[3] T. L. Linnik, A. V. Scherbakov, D. R. Yakovlev, X. Liu, J. K. Furdyna, and M. Bayer. Theory of magnetization precession induced by a picosecond strain pulse in ferromagnetic semiconductor (Ga,Mn)As. *Phys. Rev. B*, 84:214432, 2011.

[4] L. Thevenard, J.-Y. Duquesne, E. Peronne, H. J. von Bardeleben, H. Jaffres, S. Ruttala, J-M. George, A. Lemaître, and C. Gourdon. Irreversible magnetization switching using surface acoustic waves. *Phys. Rev. B*, 87:144402, 2013.

[5] P. Němec, V. Novák, N. Tesařová, E. Rozkotová, H. Reichlová, D. Butkovičová, F. Trojánek, K. Olejník, P. Malý, R.P. Campion, B.L. Gallagher, Jairo Sinova, and T. Jungwirth. The essential role of carefully optimized synthesis for elucidating intrinsic material properties of (Ga,Mn)As. *Nature Communications*, 4:1422, 2013.

[6] D Sander. The correlation between mechanical stress and magnetic anisotropy in ultrathin films. *Reports on Progress in Physics*, 62:809, 1999.

[7] D. Sander, S. Ouazi, A. Enders, Th. Gutjahr-Lőser, V.S. Stepanyuk, D.I. Bazhanov, and J. Kirschner. Stress, strain and magnetostriction in epitaxial films. *Journal of Physics: Condensed Matter*, 14:4165, 2002.

[8] R.C. O'Handley. *Modern magnetic materials: principles and applications*. John Wiley and Sons Inc., 2000.

[9] A. Mougin, C. Dufour, K. Dumesnil, and Ph. Mangin. Strain-induced magnetic anisotropy in single-crystal $RFe_2(110)$ thin films (R=Dy, Er, Tb, $Dy_{0.7}Tb_{0.3}$, Sm, Y). *Phys. Rev. B*, 62:9517, 2000.

[10] P. Kuszewski, I.S. Camara, N. Biarrotte, L. Becerra, J. von Bardeleben, W. Savero Torres, A. Lemaître, C. Gourdon, J.-Y. Duquesne, and L. Thevenard. Resonant magneto-acoustic switching: influence of rayleigh wave frequency and wavevector. *Journal of Physics: Condensed Matter*, 30:244003, 2018.

[11] M. Bombeck, A. S. Salasyuk, B. A. Glavin, A. V. Scherbakov, C. Brüggemann, D. R. Yakovlev, V. F. Sapega, X. Liu, J. K. Furdyna, A. V. Akimov, and M. Bayer. Excitation of spin waves in ferromagnetic (Ga,Mn)As layers by picosecond strain pulses. *Phys. Rev. B*, 85:195324, 2012.

[12] A. E. Clark and R. E. Strakna. Elastic constants of single crystal YIG. *J. Appl. Phys.*, 32:1172, 1961.

[13] M.J. Hurben and C.E. Patton. Theory of magnetostatic waves for in-plane magnetized anisotropic films. *Journal of Magnetism and Magnetic Materials*, 163:39, 1996.

[14] O. d'Allivy Kelly, A. Anane, R. Bernard, J. Ben Youssef, C. Hahn, A H. Molpeceres, C. Carrtro, E. Jacquet, C. Deranlot, P. Bortolotti, R. Lebourgeois, J.-C. Mage, G. de Loubens, O. Klein, V. Cros, and A. Fert. Inverse spin Hall effect in nanometer-thick yttrium iron garnet/Pt system. *Appl. Phys. Lett.*, 103:082408, 2013.

[15] P. Hansen. Anisotropy and magnetostriction of gallium-substituted yttrium iron garnet. *J. Appl. Phys.*, 45:3638, 1974.

[16] A. B. Smith and R. V. Jones. Magnetostriction constants from ferromagnetic resonance. *J. Appl. Phys.*, 34:1283, 1963.

[17] A. E. Clark, K. B. Hathaway, M. Wun-Fogle, J. B. Restorff, T. A. Lograsso, V. M. Keppens, G. Petculescu, and R. A. Taylor. Extraordinary magnetoelasticity and lattice softening in bcc Fe-Ga alloys. *J. Appl. Phys.*, 93:8621, 2003.

[18] Estimated to be 80% of pure iron magnetization.

[19] We assume a high quality sample exhibiting an iron like value of α.

[20] Measured by FMR in a 58nm thick $Fe_{80}Ga_{20}$ film.

[21] D. E. Parkes, L. R. Shelford, P. Wadley, V. Holý, M. Wang, A.T. Hindmarch, G. van der Laan, R.P. Campion, K.W. Edmonds, S.A. Cavill, and A.W. Rushforth. Magnetostrictive thin films for microwave spintronics. *Scientific Reports*, 3:2220, 2013.